LA-UR- 98-1813

Approved for public release: distribution is unlimited.

CONF-980545--

Title: **NEUTRON DETECTION AND APPLICATIONS USING A BC454/BGO ARRAY**

Author(s): **M. C. Miller, R. S. Biddle, S. C. Bourret, R. C. Byrd, N. Ensslin, W. C. Feldman, J. J. Kuropatwinski, J. L. Longmire, S. Krick, D. R. Mayo, P. A. Russo, and M. R. Sweet**

Submitted to: **1998 Symposium on Radiation Measurements and Applications
Ann Arbor, MI USA
May 12-14, 1998
(FULL PAPER)**

Los Alamos
NATIONAL LABORATORY

LA-UR-98-1813

NEUTRON DETECTION AND APPLICATIONS USING A BC454/BGO ARRAY

M. C. Miller, R. S. Biddle, S. C. Bourret, R. C. Byrd, N. Ensslin,
W. C. Feldman, J. J. Kuropatwinski, J. L. Longmire,
M. S. Krick, D. R. Mayo, P. A. Russo, and M. R. Sweet
Los Alamos National Laboratory
Los Alamos, NM 87545

1998 Symposium on Radiation Measurements
and Applications
Ann Arbor, Michigan
May 11-14, 1998

Neutron Detection and Applications Using a BC454/BGO Array

M. C. Miller, R. S. Biddle, S. C. Bourret, R. C. Byrd, N. Ensslin, W. C. Feldman, J. J. Kuropatwinski,
J. L. Longmire, M. S. Krick, D. R. Mayo, P. A. Russo, and M. R. Sweet
Los Alamos National Laboratory, P.O. Box 1663 MS E540, Los Alamos, NM 87545
(505) 667-1556, fax (505) 665-4433, mmiller@lanl.gov

Abstract

Neutron detection and multiplicity counting has been investigated using a boron-loaded plastic scintillator (BC454)/bismuth germanate (BGO) phoswich detector array. Boron-loaded plastic combines neutron moderation (H) and detection (^{10}B) at the molecular level, thereby physically coupling increasing detection efficiency and decreasing die-away time with detector volume. Separation of the phoswich response into its plastic scintillator and bismuth germanate components was accomplished on an event-by-event basis using custom integrator and timing circuits, enabling a prompt coincidence requirement between the BC454 and BGO to be used to identify neutron captures. In addition, a custom time-tag module was used to provide a time for each detector event. Time-correlation analysis was subsequently performed on the filtered event stream to obtain shift-register-type singles and doubles count rates.

1. Introduction

A Fast Neutron Coincidence Counter (FNCC) consisting of an array of 10 neutron detectors, each composed of a boron-loaded plastic scintillator (BC454*) optically coupled (phoswich arrangement) to a bismuth germanate (BGO) inorganic scintillator, has been developed. This detector array has been configured in a 4π well configuration for application as a neutron multiplicity counter. An intrinsic advantage of BC454 is the combination of neutron moderation (H) and detection (^{10}B) at the molecular level, thereby physically coupling increasing detection efficiency with decreasing die-away time as a function of detector volume. Both of these characteristics address a fundamental limitation of thermal-neutron multiplicity counters, where ^3He proportional counters are embedded in a polyethylene matrix. Addition of the BGO element allows for a coincidence requirement between the neutron-capture reaction products (α and ^7Li, whose energy is deposited locally in the BC454) and the accompanying gamma ray (478 keV) to identify neutron capture events.

Thermal multiplicity counting [1-3] is a standard assay technique used in nuclear material safeguards. This technique is based on time-correlation counting using shift-register electronics to distinguish sources of fission neutrons from other neutron sources. Counting efficiency is enhanced by moderation of the neutrons in polyethylene prior to detection by ^3He proportional counters. Because the ^3He detectors are necessarily discrete units placed in the moderator, the average neutron lifetime (die-away time) in these types of counters is ~50 μs. The practical limitation of this method is that the statistical precision degrades rapidly for doubles (D) and triples (T) because of accidental coincidence counts caused by uncorrelated neutrons, primarily from (α,n) reactions.

Previous calculations [4] have compared the assay performance of conventional thermal counters with those based on BC454 and have shown that orders of magnitude improvement in the count time required for the assay can be obtained for equivalent-efficiency systems (~50%). This improvement is the result of the much shorter die-away time for BC454 (~2 μs) coupled to the high neutron detection efficiency.

2. Detector Characteristics

First introduced by Drake, et al. [5], and subsequently reported in more detail by Feldman, et al. [6], BC454 was originally designed for the purpose of neutron spectroscopy. Neutrons enter the plastic and elastically scatter (primarily on hydrogen), thereby creating proton recoils. These proton recoils result in the production of scintillation light. Gamma rays and x-rays also cause scintillation, primarily by Compton scattering. With boron added to the plastic, neutron capture can occur by the $^{10}B(\alpha,n)^7Li$ reaction, where Q = 2.791 MeV. The first excited state of ^7Li is produced 94% of the time and decays by emission of a 478-keV gamma ray. For plastic containing 5% by weight boron (~1% ^{10}B), capture by ^{10}B will dominate the neutron absorption (>98%) with an intrinsic die-away time of ~2 μs. The reaction products (α and ^7Li) deposit their energy locally in the plastic, producing a light output of approximately 93-keV electron equivalent (keV_{ee}). The gamma ray emitted by the excited ^7Li may or may not deposit energy in the plastic. The addition of BGO to the BC454 results in a medium-resolution gamma-ray detector capability

* Bicron Corp., 12345 Kinsman Rd., Newbury, OH 44065.

being added, allowing a coincidence between the two detector elements (93 keV$_{ee}$ in the BC454 and 478 keV in the BGO) to identify a neutron capture event. Gamma-ray interactions in the outer BGO layer are primarily photoelectric absorption and Compton scattering.

Figure 1 shows a schematic of one of the BC454/BGO detector elements. The well counter is composed of 10 of these detectors, arranged end-to-end in a five-position annulus (see Fig. 2). Each detector is shielded with lead and the gaps between detector pairs are occupied by graphite inserts to enhance neutron capture through moderation. Monte Carlo simulations of this arrangement result in a neutron capture probability of 10.6%. Other configurations easily attain the 20% – 50% range [4].

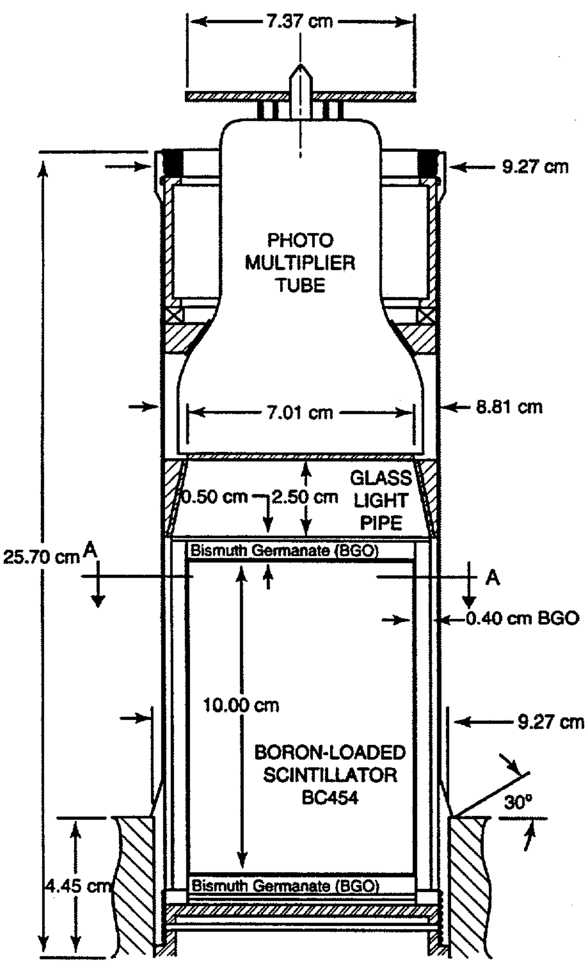

Fig. 1. Cross section of the BC454/BGO phoswich detector.

3. Data Acquisition System

A data acquisition system was developed to collect data from up to 10 of the phoswich detectors simultaneously, with the capability of handling a data

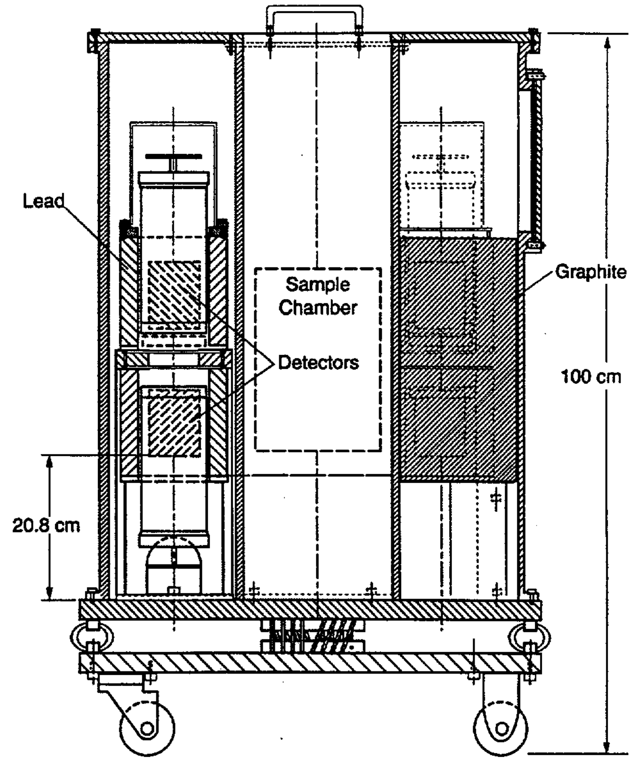

Fig. 2. Schematic of the 5-position array.

rate of 100 kHz for 1000 s. The system includes custom constant-fraction discriminator (CFD), gated-integrator (GI), and time-tag module (TTM) circuits. These electronics allow a first-order separation of the combined BC454/BGO pulse to be made as well as time-tagging each event for subsequent time-correlation analysis. The GI outputs are sent to an analog-to-digital converter (ADC) and subsequently stored in the computer. In parallel with the integration, CFD triggers are sent to the TTM providing a time stamp for each event. Analysis is done in software using the time and energy data. Figure 3 presents a block diagram of signal routing for one of the 10 detector channels.

As shown in Fig. 3, output from the preamplifier is routed to the CFD and GI electronics. The CFD/GI (including timing control logic) unit is a custom nuclear instrument module (NIM) designed and built for these experiments. As the analog signal enters the circuit, it is split, with one leg going to the CFD circuitry and the other going to the GIs. Outputs from the CFD control logic are as follows: triggers to initiate the integration of the BC454 and BGO portions of the combined signal, triggers to the TTM, and triggers to the ADC board to initiate digitization of the integrator outputs. The CFD also receives a signal from the TTM that acts to suspend CFD operation to allow

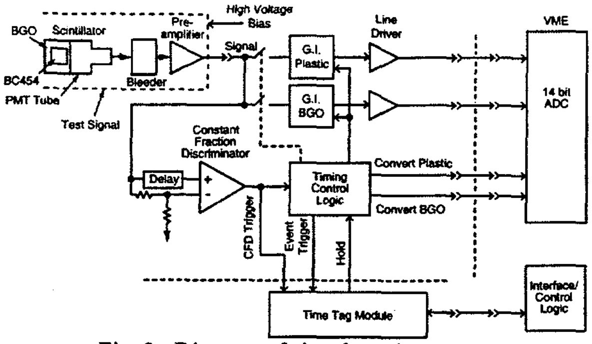

Fig. 3. Diagram of signal routing.

transfer of timing data to the computer if the TTM buffer becomes full. Integration of the signal is done by a pair of GIs. The first is open for the first 80 ns (primary BC454 component) and the second for the subsequent 400 ns (primary BGO component). The integration over the first 80-ns gate contains almost all of the BC454 and a small portion of the BGO, while the integration in the following 400-ns gate contains a majority of the BGO. Once the GIs have finished, the signal is held for 200 ns to allow sampling by the ADC. The total cycle time is 800 ns. Each CFD/GI module can accommodate a single phoswich detector.

Conversion of the output of the integrators to digital form is done by an Alphi Technology† model AD42m ADC. Each ADC has four inputs, all individually triggerable by the CFD. The model AD42m is a fast, 14-bit flash ADC with total cycle time less than that of the CFD/GI module and with on-board buffer (64 kB) capability. It is housed in a Versa Module Eurocard (VME) crate along with a 256-MB memory module (Chrisslin model 256M)‡. The AD42m and memory module reside on a local VME Subsystem Bus (VSB) to allow fast transfer of ADC data into memory. Output from the AD42m is a 16-bit word composed of 14 bits of ADC data and 2 bits of channel identifier. These 16-bit words are packed in groups of two into the 32-bit memory. Each AD42m can process data from two CFD/GI modules (two detector channels).

Event time tagging is accomplished with a custom NIM using programmable logic. The TTM receives triggers from the CFD corresponding to the event being integrated and subsequently digitized by the ADC. Time tags produced by the TTM are stored in a separate memory in a synchronous fashion with the ADC outputs, thereby allowing reconstruction of the event stream preserving both energy and time. Ten channels of input can be handled by the TTM. If other events occur during the cycle time of the integrators, the CFD sends a corresponding trigger to the TTM. A time-to-second-event is recorded for a second event, and a flag is set if two or more events occur during the cycle time. The time-tag data are written as a 32-bit word. The first 22 bits are used for recording the time of the event being integrated. This time is generated on a 4-MHz clock (250-ns resolution). The next 5 bits are used to record the time-to-second-event for any second event that occurs during the integration. A 16-MHz clock (62.5-ns resolution) is used to generate this time. The next bit is used as a flag to indicate whether or not two or more events occurred during the primary event. The last 4 bits are used for channel identification. Each channel in the time-tag module has a buffer that can store two results. If any of these buffers fills up, a hold is sent to the CFD that suspends all data processing until the buffers are emptied. A rollover (22 bits at 4 MHz) of the primary event time is recorded approximately every second, providing time continuity even during holds.

A VME parallel interface, Access Dynamics§ model DC-1 (shown in Fig. 3 as Interface/Control Logic), is used to interface the TTM to the memory module (another Chrisslin 256M) and the data-acquisition software. The DC-1 resides on a separate VSB within the same VME chassis as the ADC modules and communicates directly with the memory module. Software to control the data acquisition was created with LabWindows**, a C-based programming interface to the Windows environment and VME hardware. The data-acquisition program controls the collection of data, its retrieval from the memory modules, and collation of the energy and time data. Post processing is performed for analysis of the collected data.

4. Analysis and Results

Calibration of the BC454/BGO detector array for the quantitative assay of nuclear material based on time-correlated neutron emission rates requires the following steps:

1) The combined BC454 and BGO output pulse is separated into its component parts.
2) An energy calibration is performed for each BC454 and BGO element pair.

† Alphi Technology , 6202 S. Maple Ave. #128, Tempe, AZ 85283.

‡ Chrisslin Industries Inc., 31312 Via Colinas, Westlake, CA 91362-3905.

§ Access Dynamics Inc., 3823 Hawkins St. NE, Albuquerque, NM 87109.

** National Instruments, 6504 Bridge Point Parkway, Austin, TX 78730-5039.

3) Discrimination of neutron events is accomplished using regions of interest derived from the energy calibrations.
4) Time-correlation analysis is performed on the resulting time-tagged event stream.

The CFD/GI module performs only a first-order pulse separation of the BC454 and BGO response, with the complete separation being accomplished pulse-by-pulse during post processing. After conversion by the ADC, the digitized GI outputs of the pulse area residing within the first (short) gate, G_1, and second (long) gate, G_2, are given by

$$I_1 = f_{P1}P + f_{B1}B + O_1 \tag{1}$$

and

$$I_2 = \frac{1}{k}\left(f_{P2}P + f_{B2}B\right) + O_2 , \tag{2}$$

where

- P, B = total digitized BC454 (P) and BGO (B) pulse areas (completely integrated pulse),
- I_1, I_2 = digitized pulse integration values for the G_1 and G_2 integrator channels,
- k = relative gain for the G_1 and G_2 integrator channels,
- f_{P1}, f_{P2} = fraction of BC454 pulse area residing within the G_1 and G_2 integrator channels,
- f_{B1}, f_{B2} = fraction of BGO pulse area residing within the G_1 and G_2 integrator channels, and
- O_1, O_2 = digitized integration value of baseline offset for the G_1 and G_2 integrator channels.

If k, $f_{P1}, f_{P2}, f_{B1}, f_{B2}$, O_1, and O_2 are known, the solutions for P and B from Eqs. (1) and (2) are given by

$$P = \frac{f_{B2}\left(I_1 - O_1\right) - f_{B1}k\left(I_2 - O_2\right)}{f_{P1}f_{B2} - f_{P2}f_{B1}} = a\left(I_1 - O_1\right) - b\left(I_2 - O_2\right) \tag{3}$$

and

$$B = \frac{f_{P1}k\left(I_2 - O_2\right) - f_{P2}\left(I_1 - O_1\right)}{f_{P1}f_{B2} - f_{P2}f_{B1}} = c\left(I_2 - O_2\right) - d\left(I_1 - O_1\right) . \tag{4}$$

The relative gain k of the G_1 and G_2 was obtained by the introduction of a matched pulse pair into each preamplifier/GI combination, where the width of each pulse and the spacing between the pair were such that they fully resided within each gate.

Gate fractions of the BC454 and BGO pulses were measured experimentally using individual detectors of BC454 and BGO. Data obtained from the BC454-only and the BGO-only experiments can be used to define the fractions of each pulse in the G_1 and G_2 integration windows. Setting $B = P = 0$ in Eqs. (1) and (2), noting that the entire BC454 pulse resides within the total integration time of 480 ns, and defining X to be the fraction of the BGO pulse residing within the total integration time yields

$$f_{P1} = \frac{1}{\left(1 + \frac{k\left(I_2 - O_2\right)}{I_1 - O_1}\right)} , \tag{5}$$

$$f_{P2} = 1 - f_{P1} , \tag{6}$$

$$f_{B1} = \frac{X}{\left(1 + \frac{k\left(I_2 - O_2\right)}{I_1 - O_1}\right)} , \tag{7}$$

and

$$f_{B2} = X - f_{B1} . \tag{8}$$

Because the offsets O_1 and O_2 appear in the solutions for P and B, as well as for the pulse fractions given above, iteration is required to obtain the final values for the pulse-separation algorithm.

Energy calibration of each detector was performed with laboratory gamma-ray sources (^{137}Cs and ^{54}Mn). Once all of the calibration parameters were determined for each detector, testing of the system's neutron identification and time-correlation capabilities were accomplished by measuring a series of well-known ^{252}Cf sources. Figure 4 shows a neutron capture spectrum obtained without separation of the BC454 and BGO. The neutron capture signature is clearly seen as a peak at 93 keV$_{ee}$ (BC454) and one at 478 keV (BGO). In addition, scattering of the 478-keV gamma ray is evident. Separating the spectrum of Fig. 4 enables the prompt coincidence to be employed for neutron capture discrimination. Figure 5 shows the neutron capture spectrum after separating the BC454 and BGO components. The upper plot in Fig. 5 presents the separated BC454, showing the 93-keV$_{ee}$ peak and 404-keV edge (sum of 180° scatter of the 478-keV gamma ray and 93-keV$_{ee}$ capture peak). The lower plot in Fig. 5 shows the BGO spectrum arising from the 478-keV gamma ray. The spectra in Fig. 5 were obtained by measuring a ^{252}Cf source and applying the separation algorithm, where events of

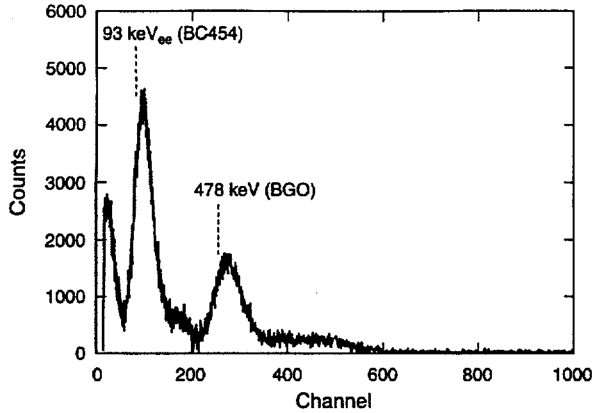

Fig. 4. Combined BC454/BGO neutron capture spectrum from ^{252}Cf.

interest were extracted by requiring a coincidence between the BC454 and BGO using a 0–400 channel region of interest (ROI) for the BC454 events and a 100–300 channel ROI for BGO events.

Measurements with the 10 detector array (FNCC) were taken for a series of well-known ^{252}Cf sources, with results given in Table I. As can been seen from Table I, the measured results are in good agreement with the known source yields (using an average efficiency obtained from the set) and compare well with measurements taken with a thermal neutron coincidence counter (TNCC). These data yield a neutron capture probability of 9.7%, compared to 10.6% as calculated by Monte Carlo simulation.

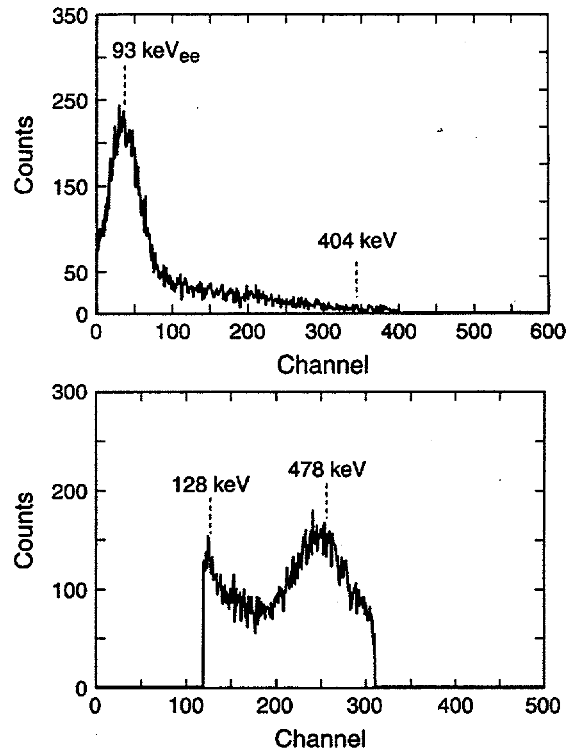

Fig. 5. Separation of the combined spectrum into its BC454 (upper) and BGO (lower) components.

Table I. ^{252}Cf Measurements- Comparison to Known Values and TNCC Data

Source ID	Known Yield (n/s)	FNCC Measured Yield (n/s)	S/S_{CF5}[1] FNCC	TNCC	D/D_{CF5}[2] FNCC	TNCC
CR5a	6352	6399	0.246	-	0.219	-
CF5	26464	26033	1.00	1.00	1.00	1.00
CF6	49752	49374	1.90	1.88	1.99	1.88
CF7	105327	105963	4.07	3.98	4.12	3.98

[1]Singles rate normalized to CF5.
[2]Doubles (coincidence) rate normalized to CF5.

5. Applications

A neutron detection system composed of BC454/BGO detectors has a variety of uses, most notably as a tool for extending nondestructive assay of special nuclear materials. As the weapons complex moves from processing and production of pure materials to waste cleanup and remediation, more and more inventory is encountered with (α,n) rates that preclude practical application of thermal neutron multiplicity counting. A high-efficiency, short die-away time system, such as that possible with BC454-based detection, would fill this void by accurately measuring these samples. In addition to traditional assay for nuclear material accountancy and protection, detectors based on BC454/BGO detectors could provide an advantage in environmental management, nonproliferation, and arms control. For example, we are currently investigating the use of these detectors for characterizing waste.

The neutron spectroscopy capability of BC454 can be exploited as a means of making energy-dependent corrections to time-correlation results, where the standard model assumes a single detection efficiency. Gamma-ray spectra collected from the BGO might be used to define the ^{240}Pu-effective fraction in measurement situations where high resolution is not required, with plutonium holdup measurements being a good example.

6. Conclusions and Future Work

Neutron detection and time-correlation analysis has been demonstrated using an array of BC454/BGO phoswich detectors. Initial results are encouraging, with good agreement obtained for a well-known set of ^{252}Cf sources. Measured rates compare well with the values expected based on computer simulations. Future work planned includes the measurement of a variety of plutonium samples with a wide range of (α,n) rates.

Acknowledgment

This work is supported by the US Department of Energy, Nonproliferation and National Security, Office of Research and Development.

References

[1] K. Böhnel, KFK2203, Karlsruhe (1975), also AWRE Translation 70 (54/4252), Aldermaston (1978).

[2] M. S. Krick and J. E. Swansen, *Nucl. Inst. Meth.* **219**, 384-393 (1984).

[3] D. M. Cifarelli and W. Hage, *Nucl. Inst. Meth.* **A251**, 550-563 (1986).

[4] M. C. Miller et al., *Appl. Radiat. Isot.* **48**(10-12) 1549 (1997).

[5] D. M. Drake, W. C. Feldman, and C. Hurlbut, *Nucl. Inst. Meth.* **A306**, 350-365 (1991).

[6] W. C. Feldman, G.F. Auchampaugh, and R.C. Byrd, *Nucl. Instr. and Meth.* **A306**, 350 (1991).